Study of Cryogenic Mechanical Strength and Fracture Behavior of Adhesives for CFRP Tanks of Reusable Launch Vehicles

Shimoda, Takayuki
Japan Aerospace Exploration Agency : Associate Senior Engineer

He, Jianmei
Japan Aerospace Exploration Agency : Associate Senior Researcher

Aso, Shigeru
Department of Aeronautics and Astronautics : Professor

http://hdl.handle.net/2324/3294

出版情報：九州大学工学紀要. 66 (1), pp.55-70, 2006-03. 九州大学大学院工学研究院

Study of Cryogenic Mechanical Strength and Fracture Behavior of Adhesives for CFRP Tanks of Reusable Launch Vehicles

by

Takayuki SHIMODA*, Jianmei HE** and Sigeru ASO***

(Received February 20, 2006)

Abstract

Bonding strengths of three types of adhesives were evaluated at different temperatures. The effects of temperature and adhesive thickness on the strength were clarified from the results. It concluded that EA9394 cured at room temperature is the overall best performing adhesive for CFRP applications at cryogenic temperatures. The initial failure mode of double-lap specimens was also discussed from the results by strain/stress analysis. And also the cryogenic fracture performance of bonded structure between CFRP using AF163-2K is examined. The tensile Mode-I and shear Mode-II fracture strengths of CFRP/AF163-2K bond joints are evaluated at room temperature and cryogenic temperature. The results indicate that both cryogenic Mode-I and Mode-II fracture strengths of CFRP/AF163-2K bond joints dropped considerably. The mismatch of coefficients of linear expansion between CFRP and AF163-2K is considered to be the primary reason. On the other hand, feasibility investigations of CFRP composite as applied to unlined CFRP cryogenic tank was conducted. Reflecting the results of the previous two phase tests on small prototype filament-wound tank conducted at room temperature and cryogenic temperature, the improved third phase of FW tank test was conducted and the result show the feasibility of CFRP tank and identified the problem to be resolved.

Keywords: Filament winding, CFRP composite, Propellant tank, Adhesive, Cryogenic, Tensile Strength, Shear Strength, FEM

1. Introduction

In the development of low-weight CFRP (carbon fiber reinforced plastics) liquid-propellant tank systems and CFRP structure for the realization of Reusable Launch Vehicles, not only the

* Associate Senior Engineer, Japan Aerospace Exploration Agency
** Associate Senior Researcher, Japan Aerospace Exploration Agency
*** Professor, Department of Aeronautics and Astronautics

cryogenic performance of adhesive bonds but also the cryogenic performance of adhesive itself becomes very important from viewpoints of the safety and durability. This is because the liquid propellants like liquid hydrogen (LH2) and liquid oxygen (LOX) have to be stored at very low temperatures: below –196°C for LH2 and near LHe temperature at -269 °C for LOX. So far not so many studies on the cryogenic performances of adhesive bonds and of the adhesive itself have been done yet, especially for lower temperature CFRP applications.

In 1991 Goeders and Perry[1)] investigated 24 types of adhesives for bonding between two adherend materials of Peek/IM-6, titanium and IM-7/8551-7(Graphite/Epoxy). They recommended using FM300 and EA9394 adhesives for metallic bonding as a result of their cryogenic investigations. A NASA contractor report by David E. Glass[2)] in Analytical Services & Materials, Inc., Hampton, Virginia, concludes that the HT435, the 340oF cure adhesive, was the superior adhesive at room temperature. The report also pointed out that EA9394, Crest3170 and PR1664 all worked for bonding stainless steel down to liquid helium temperature at -269°C. Another report of the work performed by Materials Research & Engineering, Inc. for McDonnell Douglas Space Systems, Co.[3)] indicated that EA9394 is the overall best performing adhesive for metallic applications in the lower temperature range and has the usable temperature range between -253°C and 204°C. Almost all of these investigations concluded the good results of adhesive bond strength for metal material applications at very lower temperatures.

In this study, three types of adhesive materials, FM300, HT435 and EA9394, were experimentally investigated through the double-lap tensile specimen as applied to two types of CFRP adherend materials, which we called the first test series. From the experimental results of the first test series, HT435 and EA9394 adhesives both showed relatively high cryogenic performance when bonded with different CFRP adherends. Because HT435 is an adhesive cured at a high temperature 170°C (443K), it’s not desired for CFRP application. Then the room temperature cure adhesive EA9394 is chosen as the most promising adhesive material for CFRP cryogenic applications in our study. And also, finite element modeling of the double-lap tensile specimen was executed to evaluate the bond thickness, bending effects on the strength measurements of adhesive bonds and to examine the failure modes of the double-lap tensile specimens.

On the other hand, controlling the cryogenic tensile Mode-I and shear Mode-II fracture performance of adhesively bonded joints between composite materials is very important for the safety and durability of low-weight composite tanks of liquefied propellants for launch vehicles due to the cryogenic temperatures. The substantial thermal stress-strain caused by the mismatch of thermal expansion ratios between adhesives and composites can lead to fracture strength deterioration of multiphase bonded structures, particularly at very low temperatures such as those used in cryogenics.

The cryogenic tensile Mode-I and shear Mode-II fracture behaviors of structures adhesively bonded between CFRP laminates using structural adhesive film AF163-2K were examined in this study. The structural adhesive film (AF163-2K) offers advantages, including superior resistance to high-moisture environments before and after curing, high fracture toughness and peel strength.

Lastly, the feasibility investigations[4)5)6)7)8)] of CFRP composite as applied to unlined CFRP cryogenic propellant tank for reusable vehicle systems are described. Two phases of pressurization tests on small prototype filament-wound (FW) tanks with 300mm diameter were conducted from room temperature to liquid nitrogen temperature in our previous studies. Based on the results reflection of the above-mentioned first two phases of pressurization tests, the third phase FW tank was manufactured and tested to resolve the remaining problem.

2. Mechanical Characteristics Comparison between FM300, HT435 and EA9394

2.1 The first test series for the three adhesives

2.1.1 Test configurations

In the first two test series, two kinds of CFRP flat samples (IM7-UD for first test series and T300-UD for second test series) were used as adherend materials respectively. Three types of adhesives, FM300, HT435 and EA9394, were investigated as applied to these CFRP adherends. As known FM300 and HT435 are commercial epoxy film adhesives with fixed bond thickness at 0.2mm, while EA9394 is a two-part structural paste adhesive cured at room temperature and the bond thickness need to be controlled as desired. The double-lap tensile specimen shape and size for bond strength measurements in the first two test series is shown in **Fig. 1**. For both test series, the CFRP adherend thickness was fixed at 2.0mm.

In the first test series with IM7-UD adherends, the strength measurements of adhesive bonds were measured at room temperature and -150°C of cryogenic temperature to assess the strength performance of adhesive bonds at LH2 stored temperature. Liquid nitrogen was utilized to cool down the test environment at -150°C for cryogenic temperature measurements. For EA9394 adhesive specimens, the bond thickness was uniformly controlled at 0.1mm.

In the second test series with T300-UD adherends, additional strength measurements were also executed at liquid helium temperature of -269°C to assess the strength performance of adhesive bonds at LOX stored temperature. In this test series, threads with 0.1mm diameter were used for controlling the bond thickness of EA9394 specimens to minimize the unevenness. Because the liquid helium is very difficult to be stored, special experimental equipment for liquid helium evaluation was introduced as shown in **Fig. 2**. The specimen length for all adhesives in the second test series was changed as shown in **Fig. 1** to fit the size requirement for cryostat shown in **Fig. 2**.

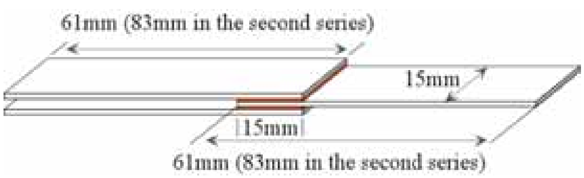

Fig. 1 Double-lap specimen in the first two test series.

Fig. 2 Cryogenic experiment.

The helium test equipment includes the test vacuum chamber (cryostat) with the test specimen loaded inside the Instron machine; the liquid helium container and a helium gas pump to push the liquid helium into the cryostat. The liquid helium will begin to be stored inside the cryostat after the vacuum chamber is cooled down to the liquid helium temperature at -269°C. The double-lap tensile tests were started after the vacuum chamber was full-filled with the liquid helium. In the liquid helium testing, the pressure of helium gas pump was controlled during the cooling process of the cryostat in order to minimize the waste of liquid helium and reduce cost.

2.1.2 Test results

The bond strengths of three types of adhesive materials as applied to two different CFRP adherend materials under different temperatures including cryogenics are experimentally obtained firstly. The results of bond strength are shown in **Fig. 3** and in **Fig. 4** for the first two test series, respectively.

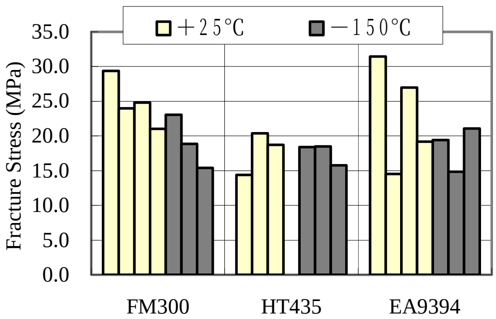

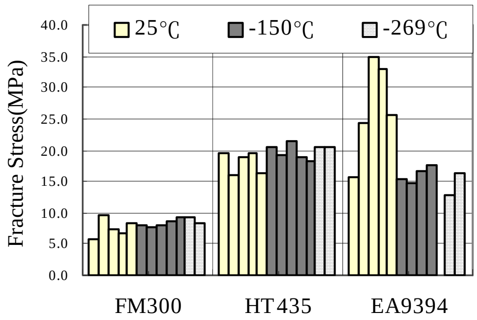

Fig. 3 Bond strength results of the first test series. **Fig. 4** Bond strength results of the second test series.

From these two figures, one can see firstly that the strength results of FM300 adhesive bond at second test series is almost half of the results from the first test series, which implies the bond strength of FM300 is very sensitive to the CFRP adherends. For HT435 and EA9394 adhesives the first two test series show relatively the same results of bond strength for different CFRP adherends. It is seen that the bond strength of HT435 and EA9394 adhesive does not get affected by the CFRP adherend like FM300 does.

Secondly one can see that both HT435 and EA9394 adhesive bonds show relatively higher performance at cryogenic temperatures as applied for different CFRP adherends. Because HT435 is an adhesive cured at a higher temperature about 170°C (443K), EA9394 adhesive cured at room temperature might be then chosen here as the more promising adhesive material for CFRP cryogenic application. More detail mechanical behaviors of EA9394, such as tensile and shear elastic modulus, tensile and shear strength etc., need to be clarified with different bond thickness at different temperatures including the cryogenic temperatures.

2.1.3 Discussions

In the first two test series, the bond strength results of all the adhesives studied here, especially for EA9394 adhesive, showed large deviations at different temperatures. Different failure behaviors at the failed surfaces are also observed from the double-lap specimens of different adhesives at different temperatures. To explain these results, the effects of adhesive bond thickness on the bond strength measurements are first discussed by comparing the strength result of EA9394 to the strength results of FM300 and HT435 adhesive bonds. And the failure behavior of double-lap tensile specimen around the adhesive/adherend bond surfaces is also discussed through the inspection of the failed surfaces.

Bond thickness effects on strength measurement: Generally speaking, the bond strength is very sensitive to all the adhesive bond thickness. Compared to commercial film adhesive FM300 and HT435, EA9394 is a two-part structural paste adhesive and it’s difficult to control the bond thickness, which means un-uniform bond thickness distribution might be easily appeared in the longitudinal and width directions of EA9394 double-lap specimen and the un-uniformity will cause bending and/or torsions which will effect the bond strength measurements. In the first test series, no attention was paid in the bond thickness of EA9394 and in the second test series we tried to control the EA9394 adhesive bond thickness at 0.1mm by using of threads with 0.1mm diameter. For FM300 and HT435 adhesive bonds, relatively small unevenness in the strength measurement results was thought coincidence with relatively uniform bond thickness because of these film adhesives.

Failure surface inspection for CFRP specimen: Because larger unevenness occurred in the strength results of the first two test series especially for EA9394 adhesive bond at room temperature, a typical failure surface pairs for EA9394 double-lap specimen at room temperature is shown in **Fig. 5**.

From this figure we can see that asymmetry of the failed surface pairs is observed for EA9394 double-lap specimen, which is not desired due to the symmetry of double-lap specimen. The asymmetry was mainly considered as the results of possible bending and/or torsion.

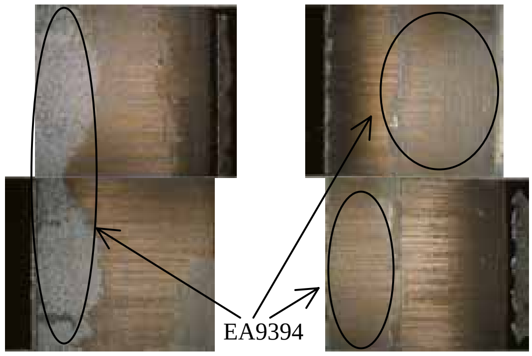

(5a) (5b)

Fig. 5 Failure surfaces of EA9394 specimen.

On one of the failed surface pair (6a), part of EA9394 adhesive bond was left on the same two sides of the bond surface, which implies that the failure initiation occurred inside EA9394 adhesive bond layer, instead of the interface between adhesive and adherend. On the other failed surface pair (6b), EA9394 adhesive is partially peeled off from one side and bonded to another side of the bond surface, which means the failure initiation occurred from the interface between EA9394 and CFRP adherend. The same phenomena can hardly be found from the results of EA9394 at cryogenic temperatures.

2.2 The second test series for EA9394 adhesive

2.2.1 Test configurations

Based on the bond strength results of the first two test series described in the previous chapter, HT435 and EA9394 adhesives showed relatively higher performance of bond strength as applied to two kinds of CFRP adherends at both room temperature and cryogenic temperatures. Because of the necessary higher temperature condition at 170°C for cure processing of HT435, EA9394 is chosen as the most promising adhesive material for CFRP cryogenic application in our study. More detail investigations to understand EA9394's mechanical behavior like elastic modulus, Poisson's ratio, tensile and shear strength etc at different temperatures need to be done.

As the third test series in this study, the shear strength of EA9394 adhesive itself was evaluated through ASTM standard D3528-96[9)]. The double-lap tensile specimen shape and size are based on the ASTM standard and also designed to fit the cryostat for liquid helium testing as shown in **Fig. 6**.

Two types of EA9394 double-lap specimen with different bond thicknesses (0.1mm and 0.2mm) are manufactured by Japan Mold System, Inc. The aluminum (AL/5020) adherend material is used following the recommendation of ASTM standard. In this series of tests, the testing temperature is also changed

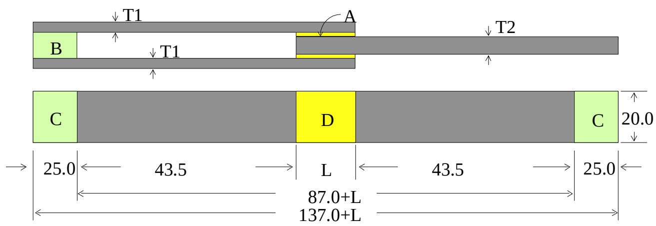

T1: 1.0 mm; T2: 2.0 mm; L: 12.7 mm

Fig. 6 Double-lap specimen based on ASTM standard.

from room temperature to two of the cryogenic temperatures: -150°C near LH2 stored temperature and LHe temperature –at 269°C near LOX stored temperature.

2.2.2 Test Results

As one part of more detail studies, investigations on the shear strength of EA9394 adhesive are also reported as the third test series of this study here. Two type of EA9394 double-lap specimen with different bond thicknesses (0.1mm and 0.2mm) are manufactured from Japan Mold System, Inc. Because experimental measurements are still now under way, only the shear strength results of 0.1mm EA9394 adhesive bond were reported here as shown in **Fig. 7** and the comparison of 0.1mm thick EA9394 adhesive bond strength of all the test series at different temperature is then shown in **Fig. 8**.

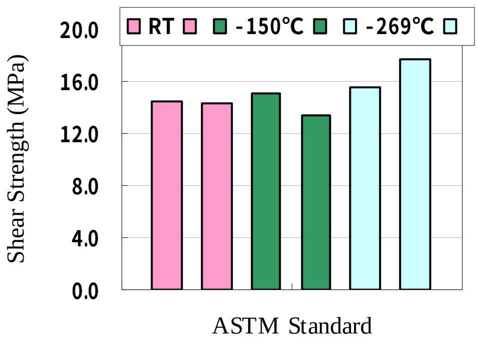

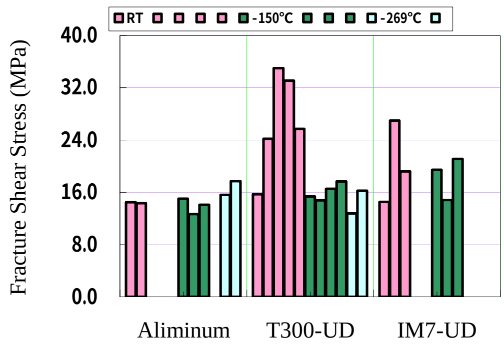

Fig. 7 Shear strength results of 0.1mm EA9394 adhesive. **Fig. 8** Comparison of EA9394 bond strength.

2.2.3 Discussions

Firstly from **Fig. 7** one can see that the shear strength of EA9394 adhesive doesn't change very much at different temperatures. This is different from the bond strength results of first two test series. The uncertainty of the strength results at this test series is also relatively smaller than at the first two test series for EA9394 adhesives. Secondly by comparing the results of EA9394 as applied for different adherend materials shown in **Fig. 8**, one can also conclude that the bond strength of EA9394 cryogenic temperatures show relatively stable results.

3. Parametric Shear Strength Study with Different Thickness for EA9394

3.1 Parametric shear strength tests

To evaluate the effect of thickness, shear strength of EA9394 adhesive were measured from room temperature to cryogenic temperature based on ASTM standards.

At first the shear strengths of EA9394 adhesive were evaluated with four types of bond thickness (0.1mm, 0.2mm, 0.5mm and 1.0mm) based on ASTM standard D3528-96[9] (Double-lap tensile test) from room temperature to cryogenic temperatures. The double-lap tensile specimen with shape and size as shown in **Fig. 6** are introduced following ASTM standard and also designed to fit the cryostat for liquid helium testing. Aluminum (AL/5020) is used as adherend material following the recommendation of ASTM standard.

Figure 9 shows the failure loads obtained from above-mentioned EA9394 double-lap tensile test at different temperatures. First of all one can see that the shear strength of EA9394 adhesive decreased with the bond thickness increased. This might be considered because of the quality inferior caused by the thicker bond. Secondly form these results we can see that the cryogenic shear strength of EA9394 adhesive almost doesn't change so much compared with the room temperature results, and for thicker bond the cryogenic shear strength becomes higher.

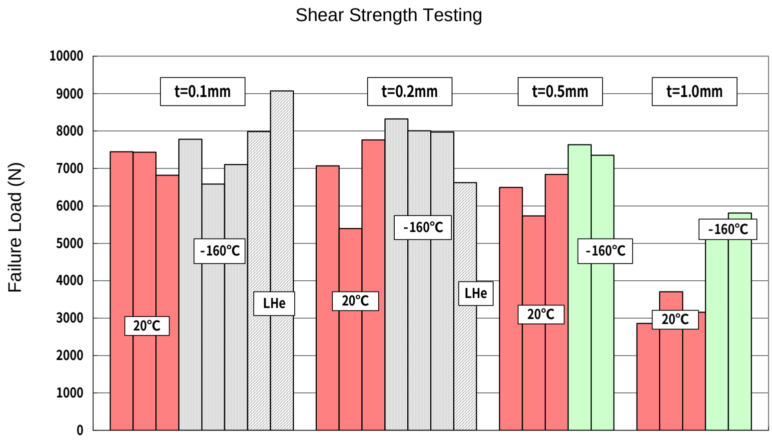

Fig. 9 Shear Strength of Bulk EA9394 Adhesive at Different Temperatures.

3.2 Finite element model analysis

The effects of bond thickness and bending on the bond strength measurements are investigated through the stress analysis to validate the double-lap tensile specimen for shear strength characterization.

The finite element analysis (FEA) is employed using the commercial soft package ANSYS to examine the effects of bond thickness and bending on the bond strength measurements, which might be induced from the misalignment of double-lap specimen during experiments. 2D plane strain approach is introduced and the full specimen is modeled as shown in **Fig. 10** because of the asymmetric loading-boundary conditions of the double-lap tensile test.

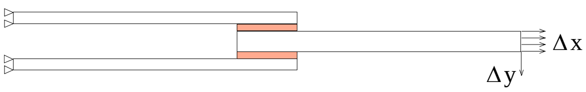

Fig. 10 Finite element modeling of double-lap specimen.

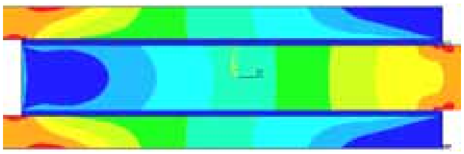

Fig. 11 Equivalent stress distribution.

The necessary input material properties are shown in **Table 1** and the model sizes are used as the same as experimental specimens of the third test series based on the ASTM standard. The finite element mesh is refined near the adhesive/adherend interfaces due to the existence of stress concentrations and free-edge effects. The EA9394 adhesive bond thickness is changed from 0.05mm to 0.3mm for parametric investigations. Displacement in thickness direction (Dy) was applied to assess the possible bending effects on the stress distributions of double-lap tensile specimen.

Figure 11 shows the typical equivalent stress distribution around the bond area of double-lap tensile specimen without any bending. From here we can see that stress concentration occurred at the interfaces between adhesives and adherend faces and these stress concentration may effect on the initiation failure mode.

Because different maximum stress component corresponding to different initial failure mode, the maximum stress components of the double-lap specimen are then calculated and shown in **Fig.12** to discuss the possible initial failure modes.

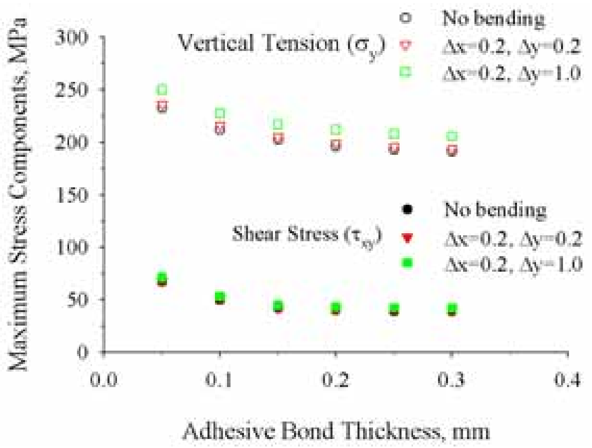

Fig. 12 Maximum stress component of EA9394 specimen.

Table 1 EA9394 and Aluminum's elastic properties.

	EA9394 (GPa)	Aluminum (GPa)
E	4.24	210.0
ν_{xy}	0.35	0.3

From this figures one can see that the normal stress component corresponding to the opening failure mode I is larger than the shear stress component corresponding to the in-plane shear failure mode II. Usually the shear strength is larger than the opening mode strength. So the failure initiation of double-lap specimen is much possible in mixed-mode than shear mode. Then one can see that possible bending will cause much higher normal stress component than shear. From these results, one can see that using double-lap tensile specimen for shear strength measurements is questionable for shear strength measurements because of the large possibility of other failure initiation mode than shear. Modification of the double-lap tensile test is needed to improve the accuracy of this test for shear strength measurements.

4. Fracture Strength Evaluation for CFRP/AF163-2K

4.1 Outline

CFRP Q-C133 prepreg sheets, made from Toho's epoxy resin #133 and reinforced by BESFIGHT IM600 were used for the adherend face materials. The following ASTM standard testing method was introduced to evaluate the Mode-I tensile fracture strengths of the Mode-I rupture energy of the CFRP/AF163-2K bond joints:

1) CFRP-Adhesive bond joints: ASTM (D5041-98) Standard Test Method for Fracture Strength in Cleavage of Adhesives in Bonded Joints[10)]

The JIS standard testing method (JIS K 7086: Testing Method for Interlaminar Fracture Toughness of Carbon Fiber Reinforced Plastics) was used for the shear Mode-II fracture strength (G_{IIC}) measurements of CFRP/AF163-2K bond joints. Testing temperatures for all experimental investigations were set at RT and cryogenic temperature (–163°C), which corresponds to the operating temperature range for liquefied natural gas propellant tanks.

Structural adhesive film AF163-2K with 0.2mm thickness, a 3M thermosetting modified epoxy structural adhesive in film available in a variety of weights with or without a supporting carrier, was utilized for the experimental study to assess the tensile Mode-I and shear Mode-II fracture behaviors of CFRP-Adhesive bond joints.

The JIS standard testing method (JIS K 7086)[11)] was used for the shear Mode-II fracture behaviors of CFRP/AF163-2K bond joints, as described below. The testing temperatures were set at

RT and cryogenic temperature of –163°C due to the operating temperature range of liquefied natural gas propellant tanks. We used a homoeothermic box for cryogenic temperature testing; liquid nitrogen was used to cool the test environment to -163°C. The homoeothermic box was completely cooled to -163°C and held at that temperature for more than 30 minutes before the cryogenic test to ensure temperature stabilization of the entire test environment, including the specimens.

4.2 Mode-I rupture energy evaluation of the CFRP/AF163-2K bond joint

4.2.1 Test configurations

The ASTM standard testing method D5041-98[10)] was used to evaluate the Mode-I rupture energy of the CFRP/AF163-2K bond structures at RT and cryogenic temperature (-163°C). Special CFRP prepreg, Q-C133, made from Toho's epoxy resin #133 and reinforced by BESFIGHT IM600 carbon fiber, was utilized as the adherend face material for this investigation. **Figure 13** displays a photograph of the specimen-loaded test environment and specimen shapes and sizes with the loading fixtures, including a wedge and an adjustable support.

The specimen width was fixed at 50mm as the optional specimen size of this standard testing method. The thickness of the CFRP laminate as the adherend face was fixed at 2.54mm. The 45o angle wedge and adjustable support fixture were made of stainless steel per ASTM recommendation. The loading speed was 127±0.5 mm/min for both temperatures, based on the standard testing method.

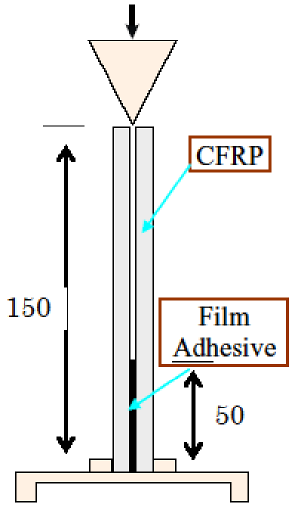

Fig. 13 Mode-I CFRP/AF163-2K bond joint testing.

4.2.2 Test results

Figure 14 depicts the loading-displacement curves obtained from room temperature testing and cryogenic temperature testing. Specimens No. 5 to No. 7 were tested at cryogenic temperature. The Mode-I energy at crack initiation and the rupture energy of the CFRP/AF163-2K bond structures were calculated from these curves; the results are displayed in **Table 2**. The cryogenic rupture energy of the CFRP/AF163-2K bond joints deteriorated to about one-fifth that at RT. The considerable thermal stresses caused by the sizable mismatch of thermal expansion ratios between the CFRP laminate and AF163-2K adhesive film were presumed to be the reason for the significant deterioration of the cryogenic bond performance of the CFRP/AF163-2K bond joints. **Figure 15** presents photographs of the failed surfaces obtained from two-temperature testing. Note that both cohesive failures and adhesive failures in the CFRP/AF163-2K bond joints occurred in RT testing, while adhesive failures occurred primarily during the cryogenic testing.

Table 2 Mode-I energies at crack initiation and failure of CFRP/AF163-2K bond joints.

Specimen	Temp.	Energy at Crack-initiation (Nm)		Failure Energy (Nm)	
CG1-01	RT	2.51	2.27±0.09	11.51	10.98±0.88
CG1-02		2.32		13.15	
CG1-03		2.12		10.21	
CG1-04		2.13		9.04	
CG1-05	-163°C	1.36	1.06±0.35	2.45	2.14±0.16
CG1-06		1.45		1.92	
CG1-07		0.37		2.05	

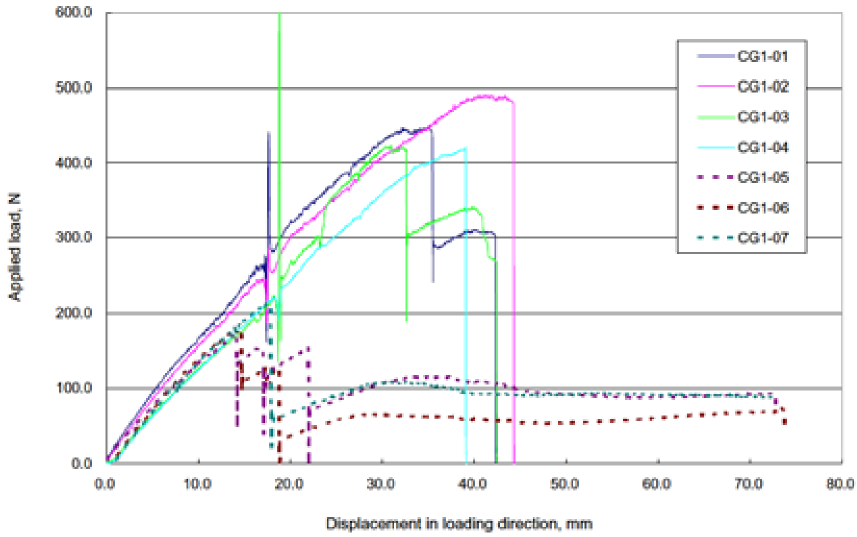

Fig. 14 Loading-displacement curves obtained from RT and cryogenic temperature testing.

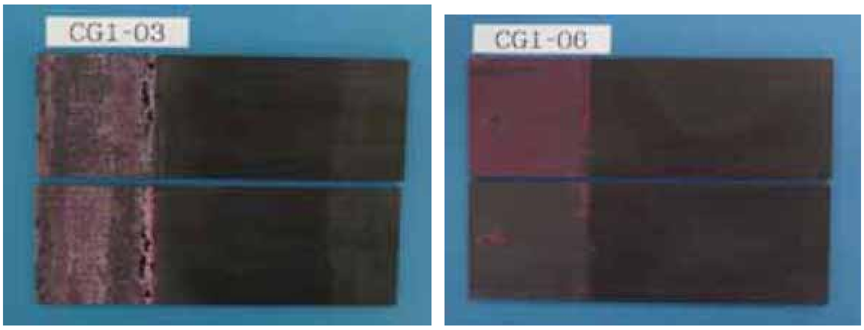

(6a) RT testing (6b) Cryogenic testing

Fig. 15 Photographs of failed surfaces for CFRP/AF163-2K bond joints.

4.3 Mode-II fracture strength evaluation for CFRP/AF163-2K

4.3.1 Test configurations

There is presently no standard testing method for Mode-II fracture toughness evaluations of adhesively bonded metal or composite bond structures. We used the JIS standard (JIS K 7086)[11] test method, also called ENF (End Notched Flexure) testing, originally established to evaluate the interlaminar fracture toughness of carbon fiber reinforced plastics, for both CFRP/AF163-2K and Al-AF163-2K bond joints.

The specimen size for CFRP/AF163-2K bond joint is provided in **Table 3**, and the loading boundary conditions of ENF testing are depicted in **Fig. 16**.

Table 3 ENF specimen sizes for CFRP/AF163-2K bond joints.

SIZE	CFRP-AF163-2K Bond Joints
L	50.0±0.1
L0	140.0±0.5
a	20.0±0.1
b	20.1±0.03
t	0.2
h	2.75±0.01

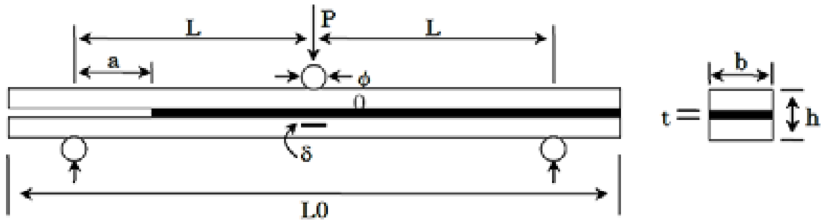

Fig. 16 ENF specimen for Mode-II fracture strength measurements.

We used micro-crack gauges (KV-25B) to monitor crack extension during the experiments. The loading speed was set at 0.5mm/min at RT, based on the JIS standard. A half loading speed at 0.25mm/min was used for cryogenic temperature testing of the CFRP/AF163-2K bond joint due to the increased bending stiffness.

4.3.2 Test results

Five specimens were tested at RT and four specimens at cryogenic temperature to assess the temperature dependence of the Mode-II fracture strength for CFRP/AF163-2K-Al bond structures. The initial critical load Pc, compliances C_0 at elastic region and C_1 at Pc load point can be calculated from the loading-displacement curves shown in **Fig. 17** which were obtained from the ENF testing at both RT and the cryogenic temperature. The Mode-II fracture toughness (G_{IIC}) of the CFRP/AF163-2K bond structures was calculated based on the JIS standard (see Appendix). The results are presented in **Table 4**. The cryogenic Mode-II fracture toughness (G_{IIC}) dropped about 60% that at RT.

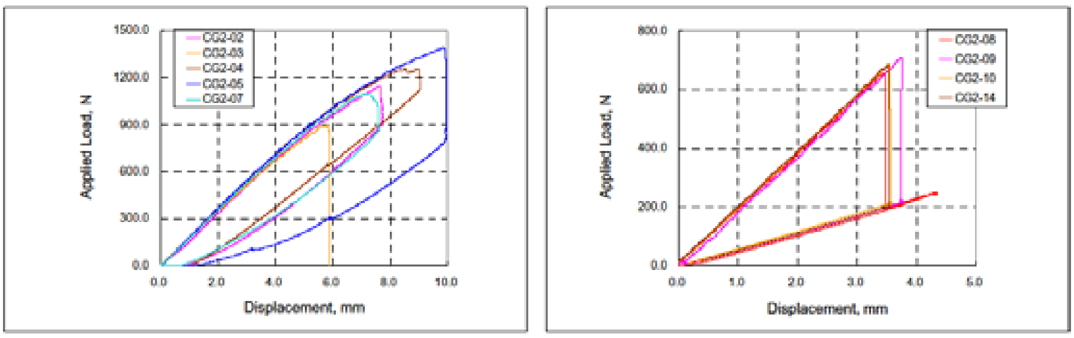

(17a) RT testing (17b) Cryogenic testing

Fig. 17 Loading–displacement curves obtained from the ENF testing of CFRP/AF163-2K bond joints.

Table 4 Mode-II fracture toughness (G_{IIC}) of CFRP/AF163-2K bond joints.

Specimen No.	Temp.	Initial Crack Length, a_0 (mm)	Initial Critical Load, Pc (5% OFFSET, N)	Compliance Elastic, C_0(mm/N)	Compliance At Pc, C_1(mm/N)	Mode-II Fracture Strength G_{II}(J/m^2)	
CG2-02	RT	20.00	1123.18	6.4E-03	6.8E-03	3953.4	2814.7 ± 711.5
CG2-03		20.00	898.06	5.7E-03	6.1E-03	2262.7	
CG2-04		20.00	1041.85	5.7E-03	6.0E-03	2999.4	
CG2-05		20.00	904.45	5.5E-03	5.8E-03	2214.7	
CG2-07		20.00	967.16	5.8E-03	6.1E-03	2643.3	
Specimen No.		Initial Crack Length, a_0 (mm)	Initial Critical Load, Pc (Maximum, N)	Compliance Elastic, C_0(mm/N)	Compliance At Pc, C_1(mm/N)	Mode-II Fracyure Strength G_{II}(J/m^2)	
CG2-08	-163°C	20.00	657.80	4.9E-03	5.3E-03	1147.2	1161.1 ±134.9
CG2-09		20.00	708.34	5.8E-03	5.3E-03	1331.4	
CG2-10		20.00	685.63	5.0E-03	5.2E-03	1001.8	
CG2-14		20.00	684.90	4.9E-03	5.2E-03	1163.8	

4.4 Conclusions

Mode-I and Mode-II fracture behaviors of CFRP/AF163-2K and Al-AF163-2K bond structures were experimentally evaluated at RT and a cryogenic temperature of -163°C in this study.

The experimental results indicated that the cryogenic Mode-I rupture energy of the CFRP/AF163-2K bond joints dropped to less than one-fifth that at RT, while the cryogenic Mode-I fracture strengths (G_{IC}) of the Al-AF163-2K bond joints dropped to half that at RT. Different failure behavior was also observed in the failed surfaces of two-bond structures at different temperatures. In contrast, the cryogenic Mode-II fracture toughness (G_{IIC}) of the Al-AF163-2K bond joints was found to decrease to about 40% that at RT, and the cryogenic Mode-II fracture toughness (G_{IIC}) dropped to about 60% that at RT for the CFRP/AF163-2K bond joints. The mismatch of thermal expansion ratios between the CFRP laminate and AF163-2K adhesive film, which exceeded that between aluminum and AF163-2K, was considered to be the primary reason for the different cryogenic fracture behavior of the two bond structures.

5. Filament Wound Proto-Type Test

5.1 History of the test series

The feasibility investigations[4)5)6)7)8)] of CFRP composite were conducted as applied to unlined CFRP cryogenic propellant tank for reusable vehicle systems. Two phases of pressurization tests on small prototype filament-wound (FW) tanks with 300mm diameter were conducted from room temperature to liquid nitrogen temperature in our previous studies. The specific CFRP material chosen was called Q-133 CFRP prepreg: which is included high-toughness and middle-elasticity epoxy resin #133 reinforced by BESFIGHT IM600.

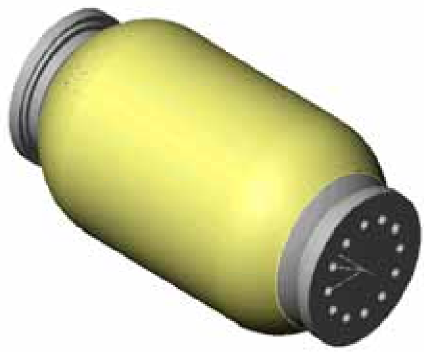

Fig. 18 Image configuration of second phase.

The first phase test of FW tank was conducted in 1999. The tank was a 300mm long cylinder with 300mm-diameter hemisphere domes at both ends. The flanges on both sides were made of SUS304 stainless steel and sealed by rubber O-rings. 10mm-width tape prepreg was used to wind on a plaster mandrel and cured in an autoclave at 180°C for 2 hours. Leakage was happened during waterproof test and the tank was cut into pieces for analyzing the weak points. The second phase test was conducted from 2001 to the beginning of 2002 and the second FW tank was manufactured with improved design and manufacturing processes. The image configuration of the improved design for second phase FW tank is shown in **Fig. 18**. The Q-133 prepreg tape was changed into 3.5mm width reflecting the investigation results of the first phase FW tank. Nickel alloy flange was used to match the thermal expansion with Q-133 CFRP. There were some large wrinkles concentrated on half surface of the completed tank (we called it unhealthy area) and the other half surface looked better which was called healthy area with some small wrinkles. Leakages were occurred at 0.3MPa pressurization test along a large wrinkle in the unhealthy area. After repairing the leakages with EA9394 adhesive, waterproof tests at room temperature with 1.0MPa and 1.5MPa internal pressures were followed on the repaired tank. After that cryogenic pressurization tests were followed with 1.5MPa and 1.9MPa internal pressures without any leakages happened in the healthy area. The first leakage in the healthy area was happened with

2.0MPa internal pressure at cryogenic temperature. Based on the detailed inspection of the cross-sectional tank wall, it concluded that the leakages were connected with the scale of wrinkles. The shrinkage of plaster mandrel during curing process and the tension control during winding were considered as the most two possible reasons for the occurrence of wrinkles and they have to be confirmed.

Based on the results reflection of the above-mentioned first two phases of pressurization tests on 300mm-diameter prototype filament-wound (FW) tanks, the third phase FW tank was manufactured to confirm that if the shrinkage of plaster mandrel during curing process would lead up to the leakages. Two-step curing process was introduced to avoid the plaster mandrel shrinkage and the tension control was kept the same with the second phase tests. It concluded that changing curing process couldn't avoid the wrinkle occurrences and the leakages were happened all over the tank surfaces during the snoop tests.

As a part of the investigations, elementary assessments on the temperature-dependence of CFRP shear performance and strength performance of the promising adhesive material EA9394 were simultaneously conducted from room temperature to cryogenic temperatures and the results were also reported here. From CFRP shear testing, the results demonstrated that shear strength of in-plane shear specimens almost doesn't change with temperature, while for inter-laminar shear the shear strength becomes higher as the temperature decreases. From EA9394 adhesive testing, we confirmed that as the temperature cooled down to cryogenics the tensile strength of EA9394 increased while the shear strength decreased.

5.2 Third phase of FW tank with different cure processing

The third phase of FW tank test was planned with the reflection of the results of the second phase tests. Here we are interested in confirming the mandrel shrinkage caused by cure processing as the main reason for wrinkle occurrences.

5.2.1 Improvement for FW tank manufacturing

Based on the investigation results obtained from the second phase test on the 300mm-diameter prototype filament-wound (FW) tank, the third phase FW tank was manufactured to confirm that if the shrinkage of plaster mandrel during cure processing would lead up to the leakages. Instead of curing the FW tank at 180°C about 2 hours, two-step cure processing was introduced trying to avoid the shrinkage of plastic mandrel during the cure processing. The detail condition of two-step cure processing was 5 hours at 140°C plus 2 hours at 180°C, which was decided after the confirmation on mandrel itself and the hardening results of CFRP prepreg. The winding angle was also changed from 30° to 37° to meet the mandrel shape design requirement. The winding pattern was [37°x2/90°x2/37°x2/90°x2/37°x2] just as same as in the second phase test. The tension control during the winding was also kept the same with the second phase

Fig. 19 The third FW tank after Cure.

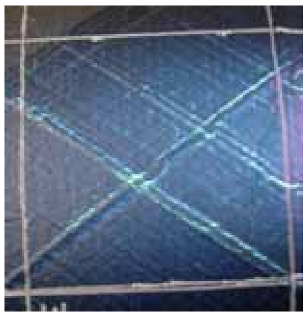

Fig. 20 Penetration test result.

tests for both helical and hoop winding the same tensile force was designed for tank manufacturing.

5.2.2 Penetration test

Figure 19 shows the photograph of third FW tank after curing process. Wrinkles were observed over the tank surface. From this point we confirmed that the wrinkles of the FW tank was not caused by the shrinkage of plastic mandrel. To assess the damages from manufacturing process, penetration test using fluorescence was firstly executed after the FW tank was completed. **Figure 20** shows one sample of the tank surface near wrinkles under fluorescence searchlight. From this test some damages were observed along the wrinkles.

5.2.3 Waterproof test at 1.0MPa

0.4MPa and 1.0MPa waterproof test was then conducted followed the penetration test. Leakages were observed over the tank surface as shown in **Fig. 21a**. To identify the leak points, we conducted snoop test and found all the leak points as shown in **Fig. 21b**. From this phase tank, leakages from the hoop winding part at the flange necks were observed for the first time. Another different point with the second phase tank was the serious leakages occurred at the interfacial area between doom and cylinder.

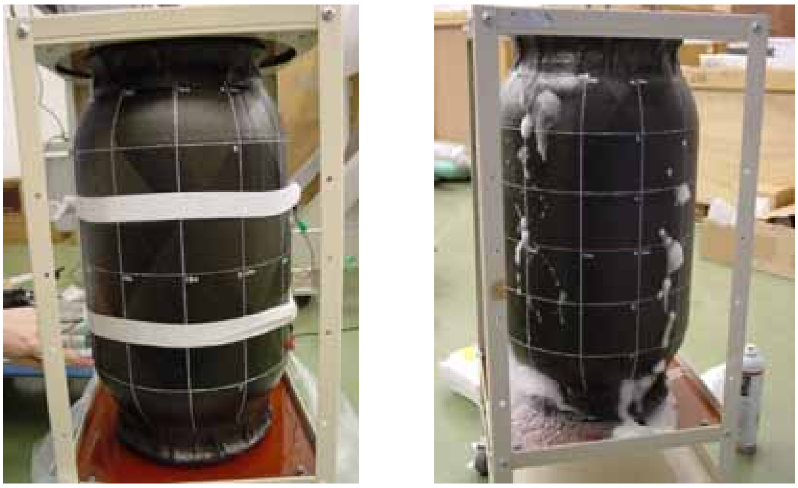

(a) Waterproof Test (b) Snoop Test

Fig. 21 Waterproof test and snoop test of FW tank.

5.2.4 Discussions

In this phase test, two-step cure processing for CFRP tank was introduced to prevent the shrink of plastic mandrel. From this point we can confirm that the shrinkage of the plastic mandrel has nothing to do with the occurrences of wrinkles over the FW tank surface. Another considerable reason for the wrinkles left was the tension control during filament winding. Because leakages from the hoop winding part at the flange necks and from the interfacial area between doom and cylinder were observed for the first time, more detail inspection of the cross-sectional tank wall need to be executed after cutting the tank to pieces.

6. Conclusion

Cryogenic performance of adhesive bonds was examined from a variety points of view and FW tank test was conducted for realizing CFRP tank of RLV. As a result, it is concluded as follows.

1. The bond strengths of three types of adhesive materials (FM300, HT435 and EA9394) are evaluated through the double-lap tensile test from room temperature to cryogenic temperatures and the effects of temperature and adhesive bond thickness are clarified.
2. It is concluded that EA9394 cured at room temperature is the overall best performing adhesive for the lower-temperature CFRP applications.
3. As one part of more detailed assessments on the mechanical behavior of EA9394 adhesive, the shear strength of EA9394 with different bond thickness at different temperatures are experimentally examined and the initial failure modes of double-lap tensile specimen are also discussed through the strain/stress analysis results to show the accuracy of the test for adhesive shear strength measurements.
4. It should be considered for designing composite vehicles that fracture strength of AF163-2K is considerably affected by cryogenic temperature
5. For FW proto-type tank test, the shrinkage of plastic mandrel during cure processing is confirmed having nothing to do with the wrinkles occurred on the FW tank surface. From the result of the proto-type tank series, positive feasibility was clarified for realizing CFRP propellant tank with improving the problem recognized in these researches.

References

1) Goeders and Perry J.L., “Adhesive Bonding Peek/IM-6 Composite for Cryogenic Applications,” 36th International SAMPE Symposium, Vol.36, pp.348-361, April 1991.
2) Glass, D. E., “Bonding and Sealing Evaluation for Cryogenic Tanks,” NASA Contractor Report 201734, Contract NAS1-96014, August 1997.
3) Anon., “Double Lap Shear and T-Peel Tests in a Temperature Range from –423oF to 350oF,” Work Performed for McDonnell Douglas Space Systems, Co. by Materials Research & Engineering, Inc., PO No. 96674005H, February 29, 1996.
4) Morimoto, T., Shimoda, T., and Morino, Y., “Cryogenic Test of CFRP Scale Tank for the Future Rocket Plane Propellant,” Proceedings of the 37th Aircraft Symposium, pp. 541-544, Tokyo, November 1999.
5) S. Cantoni, G. Di Vita, G Totaro, Morino, Y., and Morimoto, T., “Applicability of Filament Winding Method to Fabricate Cryogenic Composite Tanks for Liquid Propulsion,” IAF-00-S.3.08.
6) S. Cantoni, G. Di Vita, G. Totaro, Morino, Y., Morimoto, T., and Shimoda, T., “Cryogenic Composite Tanks for Liquid Propulsion” 2nd International Symposium Atmospheric Re-entry Vehicles and Systems, 2001, Arcachon.
7) Shimoda, T., Morino, Y., Ishikawa, T., Morimoto, T. and S. Cantoni, ”Study of CFRP Application to Cryogenic Fuel Tank for RLV,” 7th Japan International SAMPE Symposium, Tokyo, November 2001.
8) Shimoda, T., He, J., Morino, Y., Morimoto, T., ”Study of CFRP Application to Cryogenic Fuel Tank for RLV,” 23rd International Symposium on Space Technology and Science, Matsue, Japan, May 2002.
9) ASTM Standard D3528-96, “Standard Test Method for Strength Properties of Double Lap Shear Adhesive Joints by Tension Loading,” American Society for Testing and Materials, Philadelphia, September 1996.
10) ASTM (D5041-98): Standard Test Method for Fracture Strength in Cleavage of Adhesives in Bonded Joints.
11) JIS K 7086: Testing Method for Interlaminar Fracture Toughness of Carbon Fiber

Reinforced Plastics.

APPENDIX

CALCULATION OF MODE-II FRACTURE TOUGHNESS (G_{IIC}) FOR ADHESIVELY BONDED JOINTS

The mode-II fracture toughness (G_{IIC}) of adhesives in bonded metal joints can be calculated from the following equation based on (JIS K 7086) [11] (3):

$$G_{IIC} = \frac{9\alpha_1^2 P_C^2 C_1}{2B(2L^3 + 3\alpha_1^3)} \qquad (1)$$

Here, $$\alpha_1 = \left[\frac{C_1}{C_0} a_0^3 + \frac{2}{3}\left(\frac{C_1}{C_0} - 1\right) L^3 \right]^{\frac{1}{3}}$$

and

G_{IIC}: Mode-II fracture toughness

a_0: Initial crack length (mm)

P_C: Initial critical load (N)

C_1: Compliance at the PC load point (mm/N)

C_0: Compliance at the elastic region (mm/N)

α_1: Approached crack length at the PC load point (mm)

L: Half length of the span (mm)

B: Specimen width (mm)